View metadata, citation and similar papers at core.ac.uk
brought to you by CORE
provided by University of Huddersfield Repository

Effects of temperature on the ion-induced bending of germanium and silicon nanowires

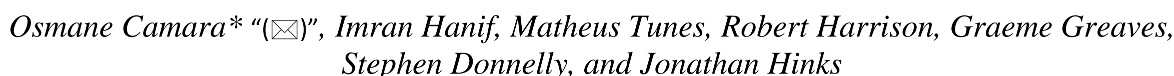
Osmane Camara "(✉)", Imran Hanif, Matheus Tunes, Robert Harrison, Graeme Greaves, Stephen Donnelly, and Jonathan Hinks*

School of Computing and Engineering, University of Huddersfield, Queensgate, Huddersfield, HD1 3DH, United Kingdom

*Corresponding author: osmane.camara@hud.ac.uk

Keywords: ion induced bending of nanowires, radiation damage, nanowires, nanomanipulation, in situ transmission electron microscopy, semiconductors, temperature

---

Abstract

Nanowires can be manipulated using an ion beam via a phenomenon known as ion-induced bending (IIB). While the mechanisms behind IIB are still the subject of debate, accumulation of point defects or amorphisation are often cited as possible driving mechanisms. Previous results in the literature on IIB of Ge and Si nanowires have shown that after irradiation the aligned nanowires are fully amorphous. Experiments were recently reported in which crystalline seeds were preserved in otherwise-amorphous ion-beam-bent Si nanowires which then facilitated solid-phase epitaxial growth (SPEG) during subsequent annealing. However, the ion-induced alignment of the nanowires was lost during the SPEG. In this work, *in situ* ion irradiations in a transmission electron microscope at 400°C and 500°C were performed on Ge and Si nanowires, respectively, to supress amorphisation and the build-up of point defects. Both the Ge and Si nanowires were found to bend during irradiation thus drawing into question the role of mechanisms based on damage accumulation under such conditions. These experiments demonstrate for the first time a simple way of realigning single-crystal Ge and Si nanowires via IIB whilst preserving their crystal structure.

1.0 Introduction

The use of nanostructured materials such as nanowires in semiconductor devices offers the possibility of satisfying or even surpassing Moore's Law and, in this context, single-crystal Ge nanowires offer considerable advantages [1], [2]. Specifically, compared to Si, its larger exciton Bohr radius (to facilitate quantum confinement), its lower temperature of recrystallization (to help reduce thermal budgets) and the higher mobility of its charge carriers (for improved device performance) make single-crystal Ge nanowires promising potential components for the next generation of field-effect transistors [1]–[5].

The manipulation of these nanostructures is currently not as trivial as handling bulk materials, although the possibility of aligning an array of nanowires during growth is currently being investigated [6]–[11]. However, the accessible configurations will likely be restricted due to the fact that the angle between the substrate and the nanowires is dependent on the crystallographic growth direction [12], [13]. Furthermore, any alignment of the nanowires that may be achieved during growth are currently lost when the nanowires are removed from their substrates. For these reasons, the development of a technique to readily manipulate nanowires after growth would be highly desirable.

Ion implantation is a standard technique used to dope semiconductors [5], [14]. It has now been well established that when applied to nanostructures, it may cause ion-induced bending (IIB). This phenomenon has been demonstrated in a wide variety of structures such as nanotubes [15], microcantilevers and nanowires [16], [17], [13], [12], [18]–[21]. With appropriate tuning of the ion beam parameters, the nanostructures can either be bent away from or towards the incoming

ion beam. The manipulation of nanostructures via IIB has been observed in many materials including Al, ZnO, Ge, Si and C [16], [17], [13], [12], [18], [19], [22].

The mechanisms behind this phenomenon are still subject of debate and different explanations for IIB have been proposed. Following their work on C nanopillars and cantilevers, Tripathi *et al.* put forward a mechanism for IIB towards the beam which was based on thermal expansion inside the target structure during irradiation [21]. Rajput *et al.* have studied metallic cantilevers, Al nanowires and polycrystalline Si nanowires [17], [20], [22]. They concluded that the bending of these structures towards the ion beam is due to dynamic "rearrangement of the disturbed atoms" at the surface facilitated by the heat deposited by the incoming ions [17]. The reconfiguration of these atoms supposedly leads to a shrinkage of the surface on which the ions are incident giving rise to a bending towards the ion beam.

Borschel *et al*[16], [19] studied ZnO and GaAs single-crystal nanowires and concluded that the differences between the distributions of self-interstitials and vacancies generated during irradiation was the cause of IIB [16], [19]. According to the authors, an excess of self-interstitials or vacancies creates volume expansion or contraction, respectively, at different depths within the nanowire. After shallow implantation and the removal via sputtering of vacancy-rich near-surface layers, there remains an excess of self-interstitials in the part of the nanowire which is closest to the direction of irradiation. Therefore, a volume expansion in this region causes the nanowire to bend away from the ion beam. For higher-energy irradiations, the distributions of the deeper self-interstitials and the shallower vacancies will be further from the surface causing an expansion and contraction, respectively, inside the nanowire which was proposed as being responsible for bending towards the ion beam.

Work on single-crystal Ge nanowires by Romano *et al.* [18], as well as on single-crystal Si nanowires by Pecora *et al.* [13], [12], pointed to amorphisation by the ion beam as the cause

behind the IIB effect. Romano *et al.* [18] proposed partial amorphisation of Ge nanowires by Ga ions as the cause of IIB away from the ion beam in the early stages of their irradiations. At these lower fluences, the authors observed that the nanowires bent away and were rendered amorphous on the side facing the ion beam whilst remaining crystalline on the opposite side. They concluded that the stress between the amorphous side and the denser crystalline side led the nanowire to bend away from the ion beam. As the irradiation was continued and the Ge nanowires became completely amorphous, the authors observed that the nanowires started to bend towards the beam and finally became fully aligned with it.

Romano *et al.* proposed two possible explanations for the bending of Ge nanowires towards an ion beam. One of these attributed the bending to an anisotropic plastic deformation known as ion hammering (also proposed by Pecora *et al.* to explain the bending of Si nanowires towards a Ge ion beam) [13], [12]. This effect is observed in amorphous materials and could cause a compressive deformation in the direction of the incoming ion beam due to an anisotropic thermal spike [13], [12], [18]. The second possibility put forward by Romano *et al.* was a densification of amorphous material under irradiation. This was based on previous studies which showed that an amorphous material might be disturbed from its relaxed state when irradiated and become denser as a result [18].

IIB towards the beam is perhaps a more-controllable direction in which to manipulate nanowires as the final orientation can be chosen simply by setting the ion beam parallel to the desired direction. As a further advantage, once parallel to the ion beam the nanowires have been observed to become straight [17], [19]. In Ge and Si nanowires, bending in the direction of the ion beam has been reported by some authors to occur only when they are fully amorphous [13], [12], [18]. Unfortunately, for most applications semiconductor nanowires operate most efficiently when single-crystal as it is in this form that their optimum electronic properties are preserved [23], [24]. Although the experiments of Romano *et al.* [18] confirmed the possibility

of aligning Ge nanowires with the ion beam, their observations also indicated that it was unlikely that a nanowire could be recovered as a single crystal via solid-phase epitaxial growth (SPEG) as they would lack the necessary crystalline seeds. Pecora *et al.* managed to retain a crystalline region at the base of tapered Si nanowires after irradiation [13], [12]. However, during subsequent SPEG from the crystalline seed the nanowires unbent and realigned to their original orientation thus losing their alignment to the ion beam direction.

Amorphisation of semiconductors during ion irradiation can be prevented by conducting the implantation at high temperatures (hot implantation). There is then no requirement for a high-temperature anneal to restore crystallinity (with the added risk of random nucleation and growth (RNG)) and the overall thermal budget can be reduced [25]–[27]. The minimum temperature chosen for hot implantation depends on many factors such as the ion species, the flux and the target material. In this paper, we present investigations of IIB of Ge and Si nanowires at temperatures high enough to prevent amorphisation during irradiation carried out *in situ* in a transmission electron microscope (TEM).

2.0 Experimental Method

Single-crystal Ge nanowires were obtained as-grown on Si wafers from Nanowire Tech Ltd (product number GNWsI15). Single-crystal Si nanowires were purchased from Sigma-Aldrich (product number 731498) in powder form. The Ge nanowires were harvested from the wafer and dispersed in ethanol using an ultrasonic bath at room temperature for 15 minutes. The Si nanowires were dispersed in an ethanol solution using an ultrasonic bath at room temperature for 90 minutes. The solutions were deposited onto 400 mesh Mo TEM grids and left to dry in air at room temperature. This sample preparation technique was designed to produce a dispersion of nanowires, once transferred onto the Mo TEM grids, such that there are tens of

nanowires visible around the edges of each grid square. It is vital to achieve this as overlapping and intertwined clusters of nanowires would render IIB irradiation experiments on individual nanowires impossible.

The Ge and Si nanowires typically had lengths ranging from 100 to 2000 nm and from 300 to 5000 nm, respectively. The Ge nanowires had diameters typically ranging between 20 and 60 nm whilst the Si nanowires ranged from 30 to 70 nm. The nanowires were randomly deposited on the TEM grids resulting in the angle, α, between the ion beam and the normal to the nanowire axis to vary.

The evolution of the orientations and microstructures of the nanowires were monitored using TEM with *in situ* ion irradiation at the Microscopes and Ion Accelerators for Materials Investigations (MIAMI) facility at the University of Huddersfield. The MIAMI-1 system used in this work consists of a JEOL JEM-2000FX TEM coupled with an ion accelerator capable of delivering inert gas ions with energies from 1 to 100 keV at an angle of 30° to the electron beam [28]. In this work, a 30 keV Xe ion beam was used to irradiate Ge nanowires and a 40 keV Xe ion beam was used for the Si nanowires. The difference in the energy selections was to achieve similar damage profiles in the two types of nanowire. In order to irradiate the nanowires without inducing amorphisation, sample heating was performed using a Gatan 652 double-tilt holder which allows tilting about its x- and y-axes. The temperatures chosen for irradiation were those at which no amorphisation was detected under the irradiation conditions as determined during preparatory experiments. Ge nanowires were irradiated with fluxes of between 1.4×10^{13} and 2.5×10^{13} ions.cm^{-2}.s^{-1} at 400°C and the Si nanowires with a flux of 4.8×10^{12} ions.cm^{-2}.s^{-1} at 500°C. The experiments were repeated using virgin samples under the same conditions at room temperature to compare with the irradiations at elevated temperatures.

Micrographs were recorded at a range of specimen holder x-tilts before and after irradiation. As the image of the nanowire is a projection onto the xy-plane of the TEM, this tilting procedure gives 3D information on the morphological evolution of the nanowires. This is important as it is possible for a nanowire to appear straight in the TEM image but the tilting will reveal any undetected bending in the z-direction as illustrated in Figure 1.

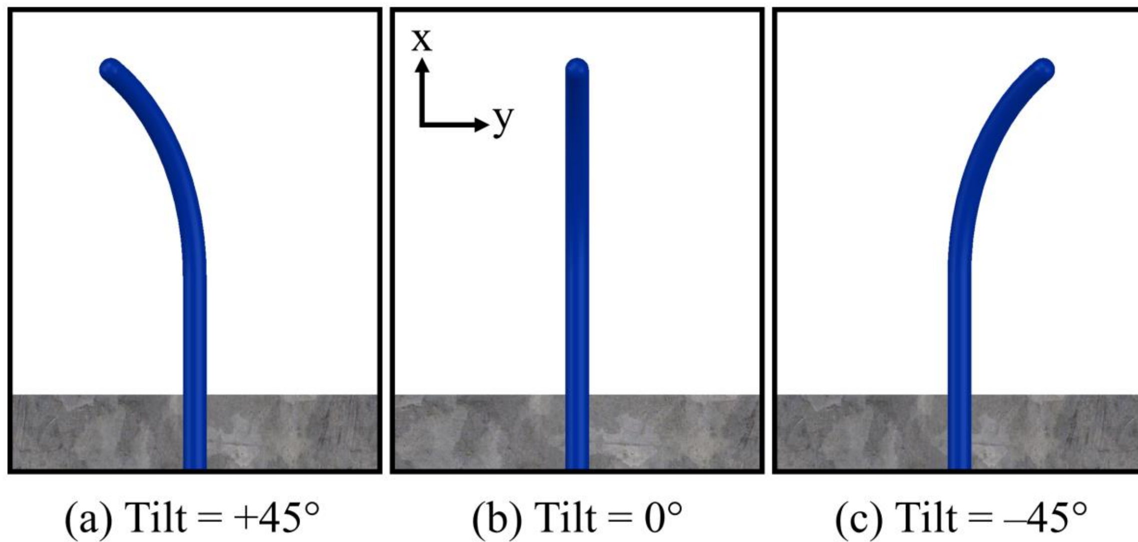

Figure 1. *Schematic showing an example of how the tilting procedure can reveal the bending of a nanowire. The nanowire is represented as it is observed in the TEM (i.e in the xy-plane of the TEM as viewed down the z-axis). (a) The nanowire appears bent towards the left when tilted by an angle of +45° on the x-tilt, (b) straight when observed at a zero tilt angle and (c) bent towards the right when tilted at –45°. In this schematic, tilting of the nanowire reveals that the nanowire is bent upwards in the z-direction. If the nanowire was bent downwards then then (a) and (c) would be reversed.*

Bright-field (BF) conditions were used to image and record videos of the nanowires before, during and after irradiation. Dark-field (DF) conditions were used to investigate structural changes within the nanowires after irradiation. Selected-area diffraction was performed on the nanowires before and after irradiation to detect crystallographic changes.

The SRIM (Stopping and Range of Ions in Matter) Monte Carlo computer code is commonly used to calculate the interaction between ions and targets [29]. However, as it calculates such interactions only for planar geometries, an algorithm called Ion Damage and RAnge in the Geometry Of Nanowires (IDRAGON) was developed to better consider the case of cylindrical nanowires. IDRAGON implements SRIM within a MATLAB environment taking into account the circular cross-section of the nanowires by cutting the cylinder into slices. A series of SRIM calculations for various thicknesses of targets were performed and then combined into the multislice model. IDRAGON was run using SRIM version 2013 in the "Detailed calculation with full damage cascades" mode for 1000 ions per slice with a displacement energy of 21 eV for Ge and 20 eV for Si[30], [31]. Values for the peak displacements per atom (dpa) were calculated from SRIM results for a depth of $\pm 0.1R$ about the Bragg peak where R is the total range of the damage.

3.0 Results and Discussion

3.1 Ion-induced bending of single-crystal Ge nanowires at elevated temperature

Bending towards the ion beam has been observed during the irradiation of Ge nanowires with 30 keV Xe at 400°C. Figure 2 shows superimposed video frames illustrating the evolution of a nanowire with increasing ion fluence and the diffraction patterns of the nanowire before and

after irradiation. The diffraction patterns do not show any significant signs of amorphisation in the irradiated nanowire and it is still a single crystal after deformation via IIB. As discussed above, amorphisation has been suggested as playing a key role in the bending of Ge and Si nanowires [13], [12], [18]. However, diffraction patterns captured at various tilt angles show that, in the experiments reported here, amorphisation of the Ge nanowires has been suppressed.

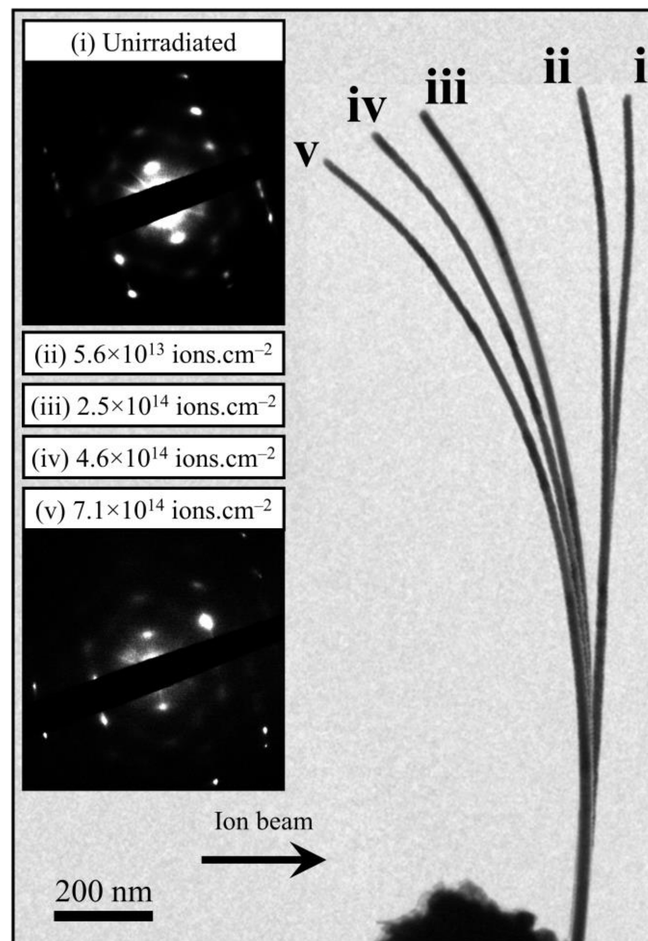

Figure 2. *Superimposed BF images from an in situ video showing the evolution of a Ge nanowire under irradiation with 30 keV Xe ions at 400°C. The nanowire, with a diameter which varied along its length from 40 and 60 nm, bent towards the ion beam and the diffraction patterns indicate that it remained crystalline. The projection of the ion beam direction onto the image plane is indicated by the arrow at the bottom of the figure.*

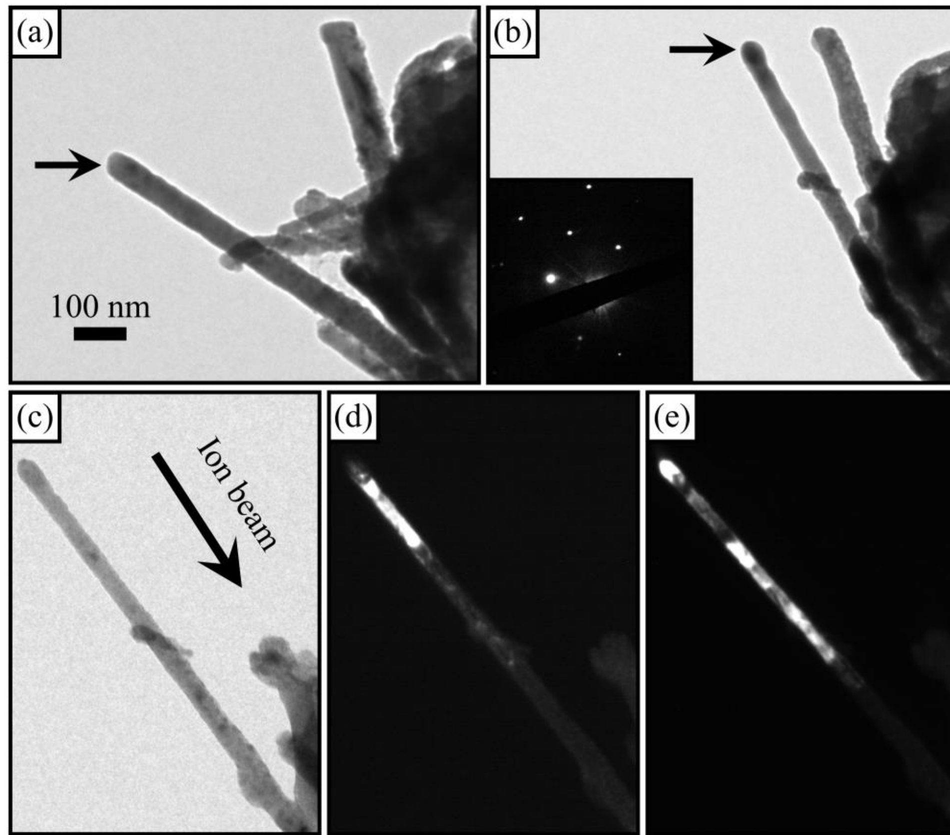

Figure 3. *The top row shows BF images of a Ge nanowire (indicated by horizontal black arrows): (a) before irradiation and (b) after irradiation with 30 keV Xe ions at 400°C to a fluence of* 2.4×10^{15} *ions.cm*$^{-2}$*. Tilting revealed that the nanowire had bent towards the irradiation. Because of the elevated temperature during irradiation, the nanowire remained crystalline as evidenced by diffraction pattern. The bottom row shows subsequent BF and DF analysis of the same nanowire after irradiation: (c) BF image, (d) DF image formed with a {004} reflection and (e) DF image formed with a {113} reflection. The DF images confirm that crystalline material is present across the whole diameter of the nanowire as expected under these irradiation conditions. It should be noted that the length of the nanowire appears significantly longer in projection in (c)–(e) compared to (a)–(b) due to tilting of the sample as described in the main text. The projection of the ion beam direction onto the image plane is*

indicated by the arrow in (c) and the scale marker in (a) applies to all the micrographs in the figure.

Figures 3(a) and 3(b) are BF images of a Ge nanowire before and after irradiation, respectively, and it can be seen that the nanowires have become thinner as a result of sputtering during the Xe ion irradiation. The nanowires are not oriented in the same manner as during the irradiation in figures 3(a) and 3(b) as they have been tilted to an angle at which the induced alignment with the ion beam was more clearly visible. A BF image of the bent nanowire after irradiation (in the same orientation as when irradiated) is presented in figure 3(c) with corresponding DF images in figures 3(d) and 3(e) which indicate that the nanowire remained crystalline after irradiation. It should be noted that in a nanowire, and especially one which is bent, not all regions would be expected to appear illuminated in a single DF image due to variations in orientation along the length of the nanowire.

3.2 Ion-induced bending of single-crystal Si nanowires at elevated temperature

Elevated-temperature IIB of single-crystal Si nanowires has also been investigated. As with the irradiation of Ge nanowires at high temperature, these experiments were performed at 500°C above the temperature at which amorphisation was found to occur in Si under the irradiation conditions used in the current work. BF images of a single-crystal Si nanowire and its diffraction patterns before and after irradiation are shown in figures 4(a) and (b). After irradiation the nanowire had bent towards the ion beam without any significant amorphisation. When Si is irradiated with Xe ions at room temperature it becomes amorphous above 0.2 dpa[32]. The nanowire shown in figure 4 was irradiated to 5.7×10^{14} ions.cm^{-2} with a peak dpa value of 3.5 dpa – more than one order of magnitude higher than the room temperature threshold for amorphisation. Thus the methods described here to align

nanowires without loss of crystallinity appear likely to be applicable to other semiconductor materials beyond Ge and Si.

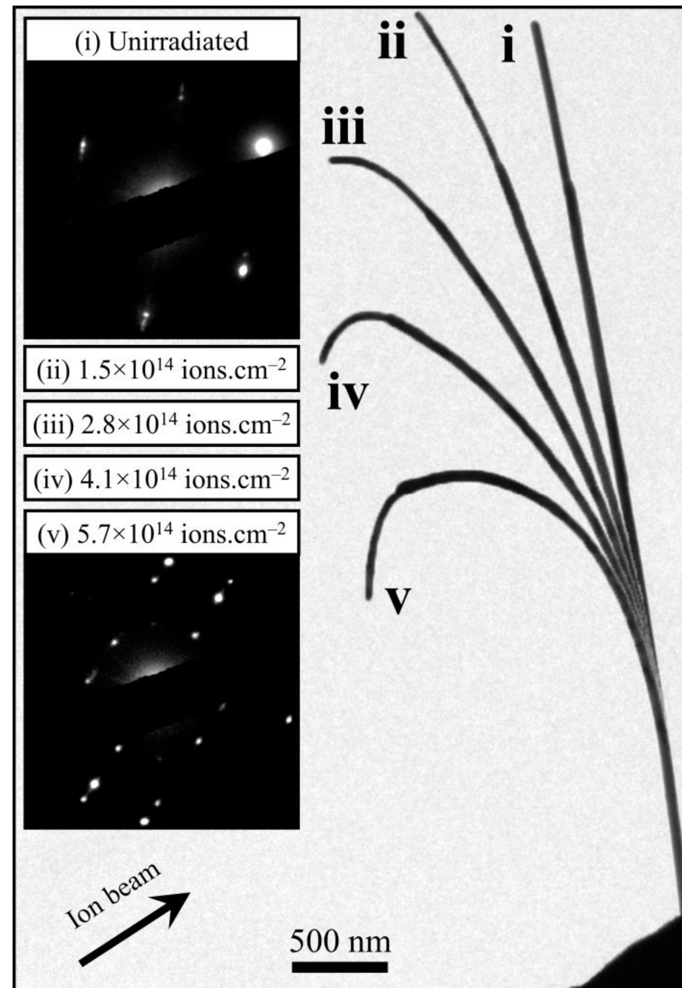

Figure 4. *Superimposed TEM images from an in situ video showing the evolution of a Si nanowire under irradiation with 30 keV Xe ions at 500°C. The nanowire, which had a diameter varying along its length from 50 and 60 nm, bent towards the ion beam and the diffraction patterns indicate that it remained crystalline. The projection of the ion beam direction onto the image plane is indicated by the arrow in the bottom left of the figure.*

3.3 IIB Mechanisms

This work has demonstrated a simple way to induce bending of Ge and Si nanowires towards an ion beam whilst retaining their crystallinity. Diffraction patterns of the nanowires were monitored during the bending and, as expected at the elevated temperatures used, remained single-crystal during the irradiations thus demonstrating that amorphisation is not required for IIB to take place.

As discussed above, Romano *et al.* [18] identified damage accumulation and more specifically amorphisation of Ge to be the driving mechanism behind IIB[18]. Similarly, Borschel *et al.* [16], [19] identified damage accumulation, and specifically the distribution of self-interstitials and vacancies within nanowires, as being responsible for volume expansion and contraction, respectively; these volume changes therefore cause bending in a direction determined by the damage depth and by the spatial separation between the interstitials and vacancies [16], [19].

Amorphisation of semiconductors occurs above a critical damage dose dependent on the irradiation conditions [3]; for Ge self-ion irradiation, this is reported to be 0.3 dpa at room temperature [28]. As heavier ions typically lead to denser atomic collision cascades and thus faster accumulation of damage, the threshold dpa at which Ge will amorphise under Xe (Z = 131) irradiation is expected to be lower than the value reported for Ge (Z = 73) ions [32], [33]. However, at 400°C at 2.7×10^{15} ions.cm^{-2} (equivalent to a peak dpa value of 35 dpa) the Ge nanowire featured in figure 6 did not show any signs of amorphisation as evidenced by the diffraction patterns. It appears that bending mechanisms based on volume changes due to damage accumulation and amorphisation are unable to explain the bending of Ge nanowires at 400°C and Si nanowires at 500°C as these processes were suppressed.

As regards the accumulation of implanted Xe within the nanowires, figures 5(a) and (b) show an example of a BF image of a Ge nanowire and its diffraction pattern before and during IIB

towards the ion beam. The results of the IDRAGON calculations presented in figure 5(c) show the implantation profile of Xe. Although $\alpha \geq 0°$ depending on the orientation of the nanowire on the TEM grid, even using $\alpha = 0°$ (in order to maximize the range of the implanted Xe) the calculations still predict that most of the ions are implanted within the side of the nanowire facing the beam. Therefore, the net effect of volume expansion due to implantation would have caused bending away from the ion beam rather than towards. Although this does not rule out implantation-induced volume change as being capable of playing a role as a competing process in the IIB of nanowires, it is clearly dominated by other mechanisms under these irradiation conditions.

Of all the mechanisms proposed to explain bending of nanowires towards an ion beam [17], [20]–[22], only those based on surface reconstruction effects and temperature gradients would appear to be valid under the experimental conditions reported here . However, the model based on temperature gradients proposed by Tripathi *et al.* is valid only for materials with a negative coefficient of thermal expansion. Since the IIB phenomenon has been observed on materials such as Ge [18], Si [13], [12], GaAs [19], ZnO [16] and Al [22], which all have positive coefficients of thermal expansion in their bulk forms [34]–[37], the results of the current work point to surface reconstruction effects as being best able to explain IIB towards an ion beam at temperatures sufficient to suppress damage accumulation. At lower temperatures at which damage accumulation can occur, such surfaces effects may similarly play a significant role in the bending phenomenon.

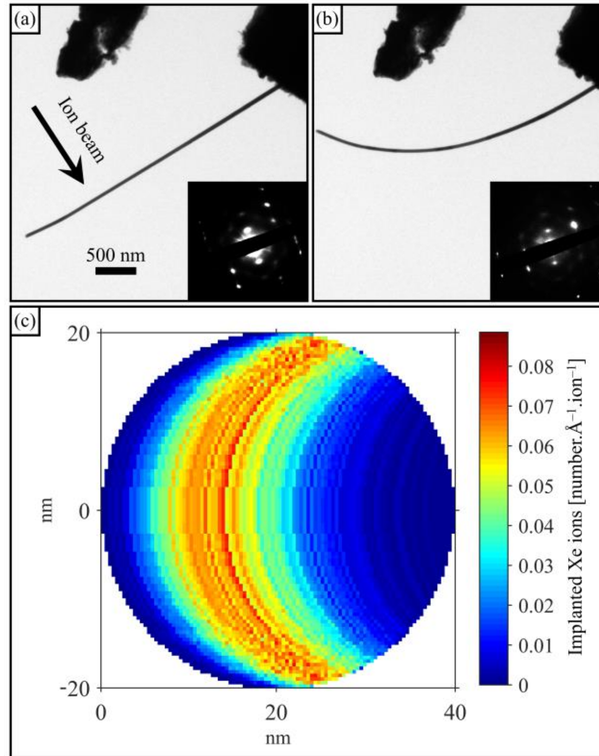

Figure 5. *TEM and IDRAGON results for 30 keV ion irradiation of a Ge nanowire at 400°C: (a) BF image and diffraction pattern before irradiation, (b) BF image and diffraction pattern after irradiation to a fluence of 7.1×10^{14} ions.cm^{-2} and (c) calculated implantation profile. The nanowire had a diameter varying along its length from 40 and 60 nm and bent towards the ion beam during irradiation. The IDRAGON calculation was performed for a diameter of 40 nm at an incidence angle normal to the nanowire axis and thus represents the maximum expected implantation depth. The projection of the ion beam direction onto the image plane is indicated by the arrow in (a) and the scale marker in (a) applies to both micrographs in the figure.*

During *in situ* experiments at 400°C on Ge nanowires in which accumulation of damage is prevented and amorphisation does not occur, only bending towards the ion beam (or no bending at all) was observed in the experiments reported here. Conversely, when the experiments were

repeated at room temperature the Ge nanowires were found to bend away from the ion beam. This failure of the nanowires to bend away from the ion beam at 400°C suggests that the mechanism(s) which favour deformation in that direction are suppressed at this temperature or that mechanism(s) which drive bending towards the ion beam are enhanced.

Figure 6(a) shows a BF image of a nanowire which has been irradiated at 400°C to a fluence of 2.7×10^{15} ions.cm^{-2}. At this relatively-high fluence, the nanowire did not bend or become amorphous. Figure 6(b) shows the BF image of the same nanowire irradiated for a second time but at room temperature. Under these conditions, the nanowire immediately started to bend away from the ion beam. It is reasonable to conclude that the high temperature during the first irradiation prevented the nanowire from bending. This again supports the arguments that mechanisms based on damage accumulation and/or amorphisation are responsible for the IIB away from the ion beam.

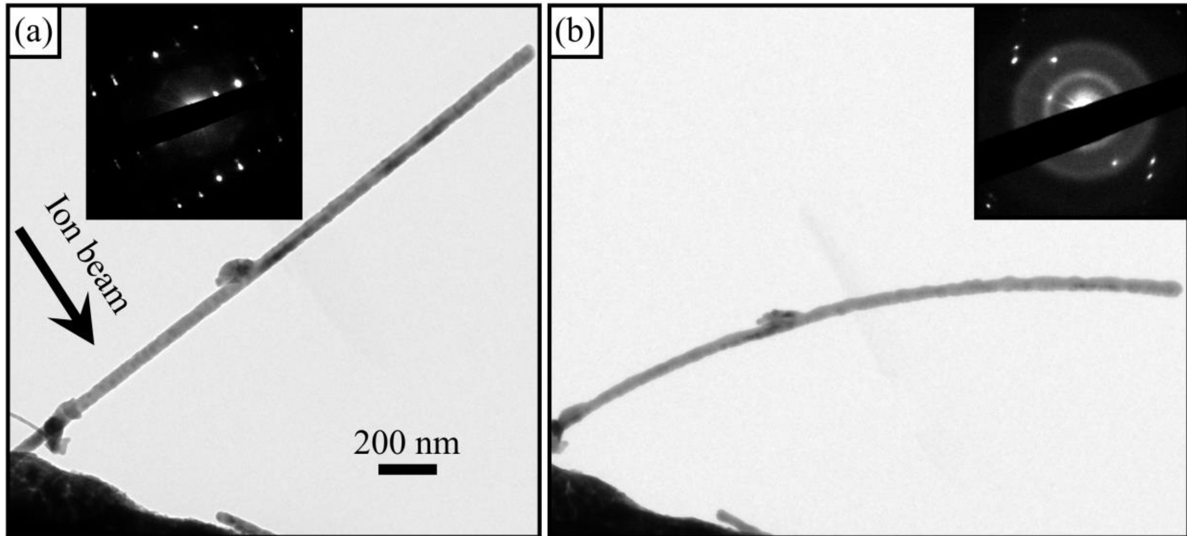

Figure 6. *BF images of a Ge nanowire: (a) after irradiation with 30 keV Xe ions to a fluence of 2.7×10*^{15} *ions.cm*$^{-2}$ *at 400°C and (b) after further irradiation to an additional fluence of 7.5×10*^{13} *ions.cm*$^{-2}$ *at room temperature with inset showing the corresponding diffraction pattern. Although no bending was observed at 400°C, the nanowire subsequently bent away from the ion beam at room temperature and the appearance of amorphous rings in the diffraction pattern demonstrates that significant damage accumulation had occurred. The projection of the ion beam direction onto the image plane is indicated by the arrow in (a) and the scale marker in (a) applies to both the micrographs in the figure.*

4.0 Conclusions

Ion-induced bending has been observed in single-crystal Ge nanowires at 400°C and Si nanowires at 500°C. Under these conditions, the nanowires remained crystalline as confirmed by both the diffraction patterns and the DF images. In addition to providing a simple way to align single-crystal nanowires, these experiments give new insights into the mechanisms which drive the bending of nanowires under ion irradiation. Of the mechanisms proposed in the literature, those based on damage accumulation and/or amorphisation have previously been

invoked in attempts to explain bending of nanowires both away from and towards an ion beam. However, it has been demonstrated in the current work that bending towards an ion beam can occur under conditions where neither significant damage accumulation nor amorphisation occur. This points towards the likelihood of surface reconstruction effects being responsible for bending towards the ion beam under irradiation at elevated temperatures as reported here. As the IIB of Ge nanowires away from the ion beam did not occur at 400°C but was observed at room temperature under otherwise identical conditions, the results of this work further suggest that different mechanisms dominate during bending away from ion beam compared to conditions under which bending is towards.

The possibility of manipulation of Ge nanowires via IIB after growth while preserving their single-crystal character has been demonstrated to be possible and the same process used for Ge nanowires has also been successfully applied to Si nanowires. This implies that the procedure reported here could be transferable to other nanostructures for which there is a requirement to preserve their crystalline character during IIB.

Acknowledgements

The construction of the MIAMI-1 facility was funded by the Engineering and Physical Sciences Research Council under grant number EP/E017266/1.

References

[1] R. A. Kelly, B. Liedke, S. Baldauf, A. Gangnaik, S. Biswas, Y. Georgiev, J. D. Holmes, M. Posselt, and N. Petkov, "Epitaxial Post-Implant Recrystallization in Germanium Nanowires," *Cryst. Growth Des.*, vol. 15, no. 9, pp. 4581–4590, 2015.

[2] S. Biswas, S. Barth, and J. D. Holmes, "Inducing imperfections in germanium nanowires," *Nano Res.*, vol. 2, pp. 1–14, 2017.

[3] A. Claverie, S. Koffel, N. Cherkashin, G. Benassayag, and P. Scheiblin, "Amorphization, recrystallization and end of range defects in germanium," *Thin Solid Films*, vol. 518, no. 9, pp. 2307–2313, 2010.

[4] D. Wang, Q. Wang, A. Javey, R. Tu, H. Dai, H. Kim, P. C. McIntyre, T. Krishnamohan, and K. C. Saraswat, "Germanium nanowire field-effect transistors with SiO2 and high-κ HfO2 gate dielectrics," *Appl. Phys. Lett.*, vol. 83, no. 12, pp. 2432–2434, 2003.

[5] R. A. Kelly, J. D. Holmes, and N. Petkov, "Visualising discrete structural transformations in germanium nanowires during ion beam irradiation and subsequent annealing.," *Nanoscale*, vol. 6, no. 21, pp. 12890–7, 2014.

[6] F. Xu, Z.-Y. Yuan, G.-H. Du, T.-Z. Ren, C. Bouvy, M. Halasa, and B.-L. Su, "Simple approach to highly oriented ZnO nanowire arrays: large-scale growth, photoluminescence and photocatalytic properties," *Nanotechnology*, vol. 17, no. 2, pp. 588–594, 2006.

[7] T. Thurn-Albrecht, J. Schotter, G. A. Kästle, N. Emley, T. Shibauchi, L. Krusin-Elbaum, K. Guarini, C. T. Black, M. T. Tuominen, and T. P. Russell, "Ultrahigh-density nanowire arrays grown in self-assembled diblock copolymer templates.,"

Science, vol. 290, no. 5499, pp. 2126–9, 2000.

[8] K. Peng, Y. Xu, Y. Wu, Y. Yan, S. T. Lee, and J. Zhu, "Aligned single-crystalline Si nanowire arrays for photovoltaic applications," *Small*, vol. 1, no. 11, pp. 1062–1067, 2005.

[9] H. J. Fan, P. Werner, and M. Zacharias, "Semiconductor nanowires: From self-organization to patterned growth," *Small*, vol. 2, no. 6, pp. 700–717, 2006.

[10] D. Wang, B. a. Sheriff, M. McAlpine, and J. R. Heath, "Development of ultra-high density silicon nanowire arrays for electronics applications," *Nano Res.*, vol. 1, no. 1, pp. 9–21, 2008.

[11] X. He, G. Meng, X. Zhu, and M. Kong, "Synthesis of vertically oriented GaN nanowires on a LiAlO2 substrate via chemical vapor deposition," *Nano Res.*, vol. 2, no. 4, pp. 321–326, 2009.

[12] E. F. Pecora, A. Irrera, S. Boninelli, L. Romano, C. Spinella, and F. Priolo, "Nanoscale amorphization, bending and recrystallization in silicon nanowires," *Appl. Phys. A Mater. Sci. Process.*, vol. 102, no. 1, pp. 13–19, 2011.

[13] E. F. Pecora, A. Irrera, and F. Priolo, "Ion beam-induced bending of silicon nanowires," *Phys. E Low-Dimensional Syst. Nanostructures*, vol. 44, no. 6, pp. 1074–1077, 2012.

[14] M. Wang, F. Ren, G. Cai, Y. Liu, S. Shen, and L. Guo, "Activating ZnO nanorod photoanodes in visible light by Cu ion implantation," *Nano Res.*, vol. 7, no. 3, pp. 353–364, 2014.

[15] B. C. Park, K. Y. Jung, W. Y. Song, B. -h. O, and S. J. Ahn, "Bending of a Carbon Nanotube in Vacuum Using a Focused Ion Beam," *Adv. Mater.*, vol. 18, no. 1, pp. 95–

98, 2006.

[16] C. Borschel, S. Spindler, D. Lerose, A. Bochmann, S. H. Christiansen, S. Nietzsche, M. Oertel, and C. Ronning, “Permanent bending and alignment of ZnO nanowires.,” *Nanotechnology*, vol. 22, no. 18, p. 185307, 2011.

[17] N. S. Rajput, Z. Tong, and X. Luo, “Investigation of ion induced bending mechanism for nanostructures,” *Mater. Res. Express*, vol. 2, no. 1, p. 15002, 2015.

[18] L. Romano, N. G. Rudawski, M. R. Holzworth, K. S. Jones, S. G. Choi, and S. T. Picraux, “Nanoscale manipulation of Ge nanowires by ion irradiation,” *J. Appl. Phys.*, vol. 106, no. 11, pp. 1–6, 2009.

[19] C. Borschel, R. Niepelt, S. Geburt, C. Gutsche, I. Regolin, W. Prost, F.-J. Tegude, D. Stichtenoth, D. Schwen, and C. Ronning, “Alignment of semiconductor nanowires using ion beams.,” *Small*, vol. 5, no. 22, pp. 2576–80, 2009.

[20] N. S. Rajput, A. Banerjee, and H. C. Verma, “Electron- and ion-beam-induced maneuvering of nanostructures: phenomenon and applications,” *Nanotechnology*, vol. 22, no. 48, p. 485302, 2011.

[21] S. K. Tripathi, N. Shukla, S. Dhamodaran, and V. N. Kulkarni, “Controlled manipulation of carbon nanopillars and cantilevers by focused ion beam.,” *Nanotechnology*, vol. 19, no. 20, p. 205302, 2008.

[22] N. S. Rajput, X. Luo, H. C. Verma, and Z. Tong, “Ion-beam-assisted fabrication and manipulation of metallic nanowires,” *Micro Nano Lett.*, vol. 10, no. 7, pp. 334–338, 2015.

[23] G. Baccarani, B. Riccò, and G. Spadini, “Transport properties of polycrystalline silicon films,” *J. Appl. Phys.*, vol. 49, no. 11, pp. 5565–5570, 1978.

[24] J. Y. W. Seto, “The electrical properties of polycrystalline silicon films,” *J. Appl. Phys.*, vol. 46, no. 12, pp. 5247–5254, 1975.

[25] F. Milési, J. Leveneur, V. Mazzocchi, F. Mazen, F. Gonzatti, K. Yckache, F. Milési, J. Leveneur, V. Mazzocchi, F. Mazen, F. Gonzatti, and K. Yckache, “High Temperature Ion Implantation Evaluation In Silicon & Germanium,” vol. 196, 2011.

[26] N. Fukata, R. Takiguchi, S. Ishida, S. Yokono, S. Hishita, and K. Murakami, “Recrystallization and reactivation of dopant atoms in ion-implanted silicon nanowires,” *ACS Nano*, vol. 6, no. 4, pp. 3278–3283, 2012.

[27] J. W. Mayer, “A COMPARISON OF THE HOT IMPLANTATION BEHAVIOR OF SEVERAL GROUP-III AND -V ELEMENTS IN Si AND Ge,” *Appl. Phys. Lett.*, vol. 11, no. 12, p. 365, 1967.

[28] J. a. Hinks, J. a. van den Berg, and S. E. Donnelly, “MIAMI: Microscope and ion accelerator for materials investigations,” *J. Vac. Sci. Technol. A Vacuum, Surfaces, Film.*, vol. 29, no. 2, p. 21003, 2011.

[29] J. F. Ziegler, M. D. Ziegler, and J. P. Biersack, “SRIM - The stopping and range of ions in matter (2010),” *Nucl. Instruments Methods Phys. Res. Sect. B Beam Interact. with Mater. Atoms*, vol. 268, no. 11–12, pp. 1818–1823, 2010.

[30] E. Holmström, K. Nordlund, and A. Kuronen, “Threshold defect production in germanium determined by density functional theory molecular dynamics simulations,” *Phys. Scr.*, vol. 81, no. 3, 2010.

[31] E. Holmström, A. Kuronen, and K. Nordlund, “Threshold defect production in silicon determined by density functional theory molecular dynamics simulations,” *Phys. Rev. B - Condens. Matter Mater. Phys.*, vol. 78, no. 4, pp. 1–6, 2008.

[32] P. D. Edmondson, K. J. Abrams, J. A. Hinks, G. Greaves, C. J. Pawley, I. Hanif, and S. E. Donnelly, “An in situ transmission electron microscopy study of the ion irradiation induced amorphisation of silicon by He and Xe,” *Scr. Mater.*, vol. 113, pp. 190–193, 2016.

[33] L. Pelaz, L. A. Marqús, and J. Barbolla, “Ion-beam-induced amorphization and recrystallization in silicon,” *J. Appl. Phys.*, vol. 96, no. 11, pp. 5947–5976, 2004.

[34] G. A. Slack and S. F. Bartram, “Thermal expansion of some diamondlike crystals,” *J. Appl. Phys.*, vol. 46, no. 1, pp. 89–98, 1975.

[35] V. M. Glazov and A. S. Pashinkin, “Thermal expansion and heat capacity of GaAs and InAs,” *Inorg. Mater.*, vol. 36, no. 3, pp. 225–231, 2000.

[36] F. C. Nix and D. MacNair, “The thermal expansion of pure metals: Copper, gold, aluminum, nickel, and iron,” *Phys. Rev.*, vol. 60, no. 8, pp. 597–605, 1941.

[37] H. Ibach, “Thermal Expansion of Silicon and Zinc Oxide (II),” *Phys. Status Solidi*, vol. 33, no. 1, pp. 257–265, 1969.